Materials Research Proceedings 69 (2026) 1240-1245 https://doi.org/10.21741/9781644904251-214

Global–Local Optimization of Composite Structures Using Unified High-Order Finite Element Models

Alex Pereira do Prado[1,2,3,a *], Dario Zamani[1,b], Alfonso Pagani [1,c], Erasmo Carrera[1,d], Saullo G. P. Castro[2,e], Roeland De Breuker[2,f], Pedro Higino Cabral[3,g]

[1]MUL 2 Lab, Department of Mechanical and Aerospace Engineering, Politecnico di Torino, Corso Duca degli Abruzzi 24, 10129 Turin, Italy

[2]Department of Aerospace Structures and Materials, Faculty of Aerospace Engineering, Delft University of Technology, Kluyverweg 1, 2629 HS Delft, The Netherlands

[3]R&D Department, Embraer S.A., Av. Brigadeiro Faria Lima 2170, 12227-901 São José dos Campos, Brazil

[a]A.PereiradoPrado@tudelft.nl, [b]dario.zamani@polito.it, [c]alfonso.pagani@polito.it, [d]erasmo.carrera@polito.it, [e]S.G.P.Castro@tudelft.nl, [f]R.DeBreuker@tudelft.nl, [g]pedro.cabral@embraer.com.br

Keywords: Structural Optimization, Composite Materials, Global–Local, Carrera Unified Formulation, Multi-Fidelity Modeling

Abstract. A global optimization framework with global–local verification is developed for composite wings by coupling a NASTRAN-based global finite element model with Carrera Unified Formulation (CUF)-based high-order local analyses. The proposed methodology enables the minimization of structural weight under stress and buckling constraints, while identifying critical zones of interest for multi-fidelity and hierarchical strategy. The global model based on first-order shear deformation theory identifies the critical regions where the CUF Equivalent Single Layer and Layer-Wise refinements should be introduced to provide detailed local buckling and stress analyses. This integrated global-local framework enables adaptive local fidelity global-local analysis, improving margins of accuracy while mapping the accessible design space and maintaining computational efficiency.

Introduction

The optimization of composite aircraft wings has long been a key challenge in aerospace structural design. Classical approaches have focused on minimizing mass or maximizing stiffness by tailoring stacking sequences and fiber orientations, often under constraints on strength, buckling, and aeroelastic performance [1–3]. These methods, implemented within commercial Finite Element (FE) solvers, have proven effective for global-level optimization but are typically limited by simplified structural theories, which are unable to represent local behaviors, especially in regions of complex stress or instability. In this regard, refined structural theories based on the Carrera Unified Formulation (CUF) [4] have been developed. CUF provides a hierarchical framework capable of generating both Equivalent Single Layer (ESL) and Layer-Wise (LW) FE formulations with Node-Dependent Kinematic (NDK). This enables an accurate representation of transverse shear effects, local buckling, and through-the-thickness stress distributions, which are critical in composite structures. CUF-based analyses have been successfully applied to a wide range of problems, including failure onset, progressive failure, and nonlinear postbuckling behavior, offering substantial improvements in accuracy over models based on Classical Laminated Plate Theory (CLPT) or First-Order Shear Deformation Theory (FSDT).

Materials Research Proceedings 69 (2026) 1240-1245 https://doi.org/10.21741/9781644904251-214

Recent studies have explored global–local strategies that combine the efficiency of global FE models with the accuracy of CUF-based structural theories [5–6]. The global model captures the overall behavior of the structure and provides the boundary conditions for high-fidelity CUF submodels, enabling precise local stress evaluations where complex stress or instability phenomena occur. When integrated with an optimization process, this approach allows adaptive fidelity across automatically detected zone of interests (ZOI), ensuring accuracy only where needed while preserving computational efficiency [7]. The present work extends this concept to a fully integrated global–local analysis framework that couples NASTRAN global optimization analyses with CUF-based refinements for the weight optimization of composite wings under stress and buckling constraints.

Methodology

The framework developed in this work is presented in Figure 1. Its objective is to minimize structural weight while satisfying stress and buckling constraints, enabling automatic Global–Local (G–L) refinement on ZOIs. The approach integrates commercial and high-fidelity numerical tools, leveraging automatic multi-fidelity, multi-model and hierarchical strategy analysis for margin verification.

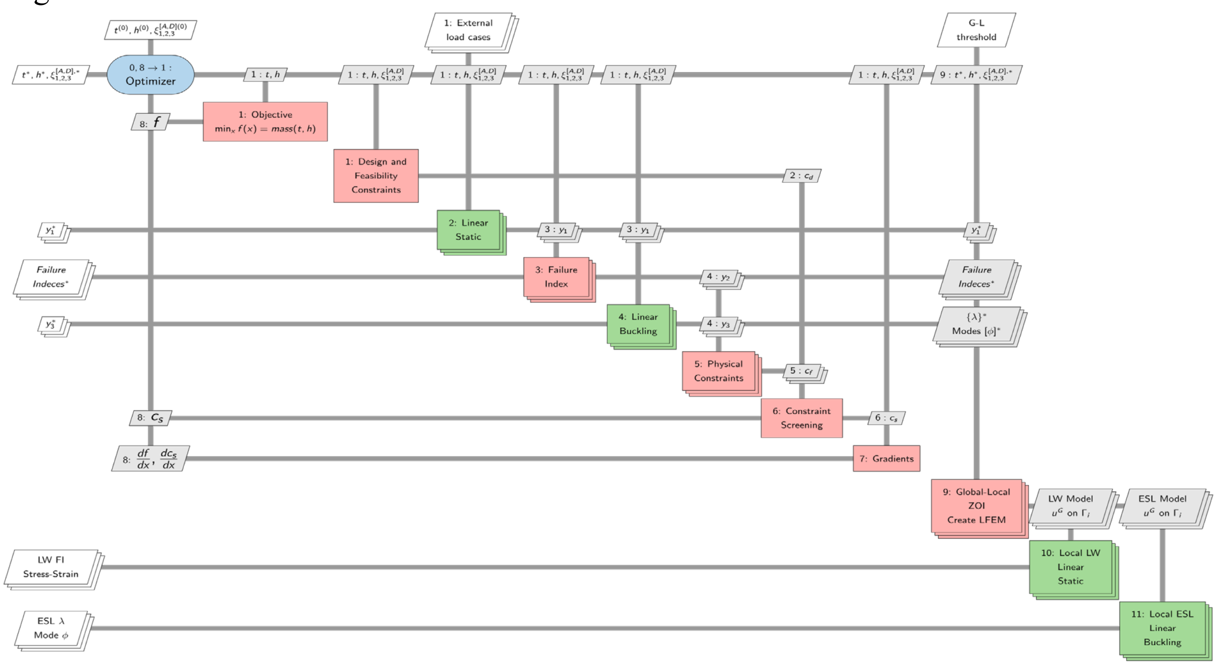

Figure 1- xDSM diagram of the novel global optimization framework with automatic global–local high-fidelity margins verification for composite structures.

In Figure 1, blocks along the diagonal represent processes, whereas off-diagonal blocks indicate the information exchanged among processes. Red blocks denote generic processes and green ones refer to FE and CUF solvers. Parallelograms represent data inputs and outputs; vertical lines indicate data-input and horizontal lines data-output. Stacked blocks denote parallel execution, and asterisks identifies optimal values.

Optimization Framework. First, a global FE model of the entire structure is built in NASTRAN using classical CQUAD4 shell elements based on FSDT. This global model serves as a computationally efficient baseline for the iterative optimization process using lamination parameters strategy [8–10]. The global optimization employs lamination parameters to map discrete stacking sequences into a continuous domain, enabling gradient-based SUMT optimization in NASTRAN MSCADS [11]. Design variables include laminate thicknesses, lamination parameters, and component shapes, while constraints comprise Angle-Minus-Loaded

Materials Research Proceedings 69 (2026) 1240-1245 https://doi.org/10.21741/9781644904251-214

(AML) failure indices [12-13], buckling loads, and laminate design and feasibility conditions [14-15]. Boundary conditions and multiple load cases are simultaneously applied to an idealized global model.

Global–Local Coupling. Second, once converged, the optimized model is automatically transferred to the G–L stage, which identifies ZOIs, extracts boundary conditions, approximates stacking sequences by minimizing AML values and ply-volume fractions using precomputed lookup tables, and generates corresponding high-fidelity CUF models.

Identification of Critical Regions. Third, ZOIs are selected through threshold criteria on AML failure indices for strength-critical elements and on global buckling-load factors followed by normalized buckling-mode displacement for buckling-critical panels. These metrics determine which regions require high-fidelity CUF analyses to verify margins and adjust the design, directly influencing final structural weight.

Local Analysis. Fourth, high-fidelity analyses are performed using the CUF, in the most critical subregions (ZOIs), allowing for an accurate evaluation of local stress and buckling behavior with an integrated G-L analysis. In the local CUF models, stress and strain distributions through the thickness, interlaminar behavior, and local buckling eigenmodes are evaluated for accurate failure-mechanism characterization.

The CUF model for the local domain adopts a displacement-based formulation, where only translational Degrees of Freedom (DOFs) are considered. Since the global model provides both translations $\left(\boldsymbol{u_x^0}, \boldsymbol{u_y^0}, \boldsymbol{u_z^0}\right)$ and rotations $\left(\boldsymbol{\theta_x^0}, \boldsymbol{\theta_y^0}, \boldsymbol{\theta_z^0}\right)$, a conversion procedure is required to express the latter as equivalent displacements. The Reissner–Mindlin displacement field in Eq. 1 is used to compute translational boundary displacements of the local model, written as:

$$
\begin{aligned}
u_x(x,y,z) &= u_x^0(x,y) + z\theta_y^0(x,y) - y\theta_z^0(x,y) \\
u_y(x,y,z) &= u_y^0(x,y) - z\theta_x^0(x,y) + x\theta_z^0(x,y) \\
u_z(x,y,z) &= u_z^0(x,y) - y\theta_x^0(x,y) + x\theta_y^0(x,y)
\end{aligned}
\tag{1}
$$

The graphical representation of these transformations is shown in Fig. 2.

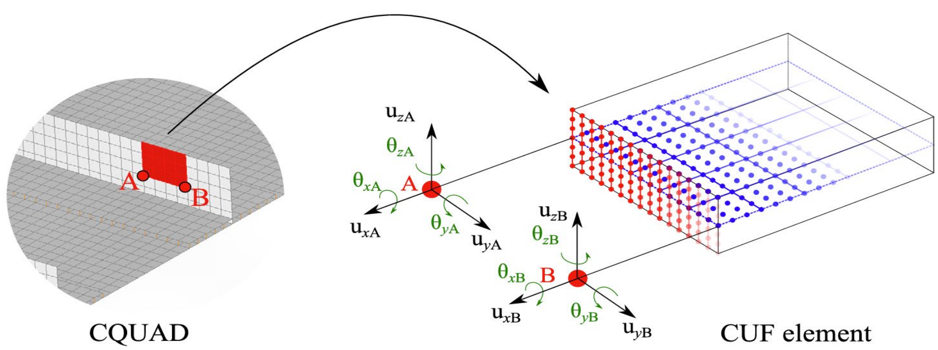

Figure 2. Schematic representation of the procedure adopted to transfer the rotational degrees of freedom from the global model into displacement-based boundary conditions for the local model.

In addition to the Element-Wise (EW) coupling strategy described above, a Patch-Wise (PW) formulation has been implemented to improve the accuracy of the boundary condition transfer between global and local models. In the EW approach, translational and rotational quantities are extracted from a single CQUAD4 element of the global model and employed to define the boundary displacements of the local CUF domain. Conversely, in the PW formulation, the interface displacements are evaluated over a larger region. This extended interpolation domain allows the contribution of all involved global nodes to be considered, resulting in smoother and more consistent boundary conditions for the local problem. The PW procedure refines the displacement field without altering the geometry of the local region, providing higher fidelity in the transfer of boundary information. This enhancement leads to more accurate local stress predictions between the global and CUF-based submodels, particularly in zones characterized by high stress gradients or local instabilities.

Results

To demonstrate the proposed framework, a simplified composite wingbox segment was modeled in NASTRAN to represent a highly loaded wing section. The model consists of ten ribs (nine bays), two spars, and upper and lower reinforced skins with five blade-shaped stringers each. The main dimensions are 6.48 m span, 1.44 m chord, and 0.29 m height. The upper and lower skins are subdivided into 54 panels, and the spars into 9 panels, all designed as symmetric and balanced laminates. Stringer webs and feet are divided into nine segments with constant lamination parameters; only thicknesses and geometries are optimized. The stringers use a constant AML parameter of –10%, representing a "hard" laminate [12–13].

Material properties correspond to Hexcel 8552 IM7 unidirectional prepreg [16], using low-temperature dry (LTD) elastic data and open-hole tension/compression (OHT/OHC) allowable considering environmental variability.

The optimization problem comprises 1,072 design variables (thicknesses, lamination parameters, stringer shapes) and 3,554 constraints related to AML failure indices, buckling loads, and laminate feasibility. Two load cases, +2.5 G and –1.0 G, are applied by scaling the nominal distributed pressure and tip loads. Boundary conditions include a clamped root, 12,081 Pa pressure on the upper skin, and tip loads of 193,047 N and –581,201 Nm, representing the running loads of the adjacent wing segment for a MTOW of 62,500 kg.

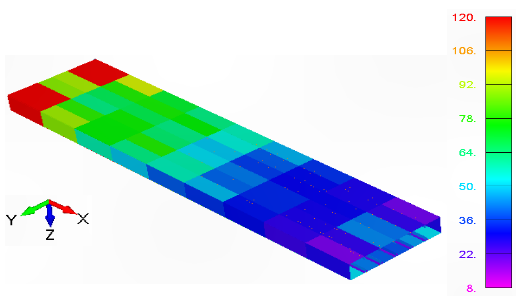

Figure 3. Optimized ply count.

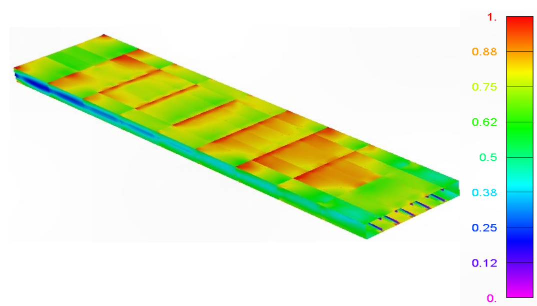

Figure 4. AML failure index.

As shown in Fig. 3, the optimization yields the number of layers, and Fig. 4 presents the corresponding AML failure indices. The optimized lamination parameters for each laminate— not shown here—contain information on fiber fractions for each lamination direction and the homogenized characteristics of the idealized optimal laminate using FSDT. This information is used to approximate stacking sequences by minimizing AML values and ply-volume fractions using precomputed lookup tables, as explained in the Methodology.

A higher number of layers improves the likelihood of obtaining a close approximation between the lamination parameters from continuous optimization and the discrete stacking sequence with similar characteristics. However, deriving an equivalent stacking sequence from idealized lamination parameters inherently introduces deviations. The effect of these deviations can be quantified by replacing panels represented by lamination parameters with discrete approximations that satisfy laminate-formation constraints and evaluating the model again.

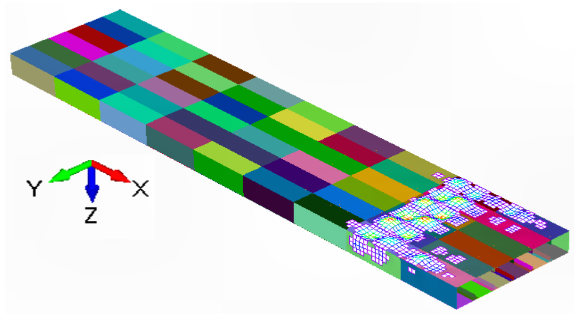

Figure 5. ZOI detection for buckled panels (5% threshold).

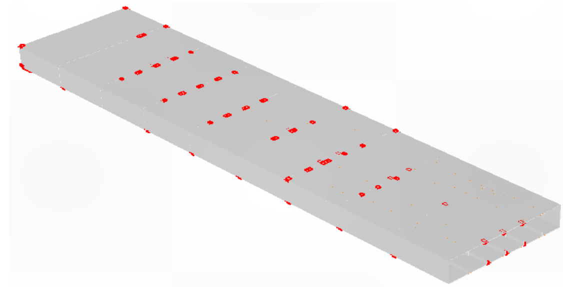

Figure 6. ZOI detection for LW stress analysis (1% FI threshold).

In this work, the G–L phase detected 25 panels out of 216 for CUF ESL buckling analysis above a 5% modal displacement threshold (Figure 5), and 191 ZOIs out of 18,900 elements for CUF LW stress analysis using a 1% AML failure index threshold (Figure 6). As an example, a critical panel with 28 layers exhibited differences of approximately 2.7% in critical buckling and 2.6% in the critical failure-index element.

Conclusions

The proposed framework integrates NASTRAN global analyses with CUF-based local refinements through a hierarchical two-level strategy for composite wing optimization. ESL models are used for local buckling assessment, while LW formulations enable detailed ply-level stress evaluation. The coupling between commercial and in-house solvers is fully automated thought ZOI detection, approximation from laminate variables to discrete stacking sequence while ensuring adaptive local fidelity during the design process. This multi-fidelity and hierarchical approach enhance constraint margins verification at two levels of local scale, explore the feasible design space with greater confidence, and maintains computational efficiency. The framework's modular architecture and high degree of automation make it suitable for integration into industrial design environments.

Acknowledgments

The authors would like to thank Daniele Scano and Professors Enrico Zappino and Riccardo Augello from the Politecnico di Torino MUL² Group for their support with the CUF formulation, modeling, and software application.

References

[1] G. Kennedy & J.R.R.A. Martins, A Comparison of Metallic and Composite Aircraft Wings Using Aerostructural Design Optimization, 12th AIAA Aviation Technology, Integration, and Operations (ATIO) Conference & 14th AIAA/ISSMO MDO Conference, 2012.

[2] D. Zamani, A. Pagani, M. Petrolo, E. Carrera. Multi-patch hybrid optimization of composite wings. III ECCOMAS Thematic Conference on Multidisciplinary Design Optimization of Aerospace Systems ,Lisbon, 22-24 April, 2025.

[3] A. Pagani, A. R. Sánchez-Majano, D. Zamani, M. Petrolo, E. Carrera: Fundamental frequency layer-wise optimization of tow-steered composites considering gaps and overlaps. Aerotecnica Missili e Spazio (2024).

[4] E. Carrera, M. Cinefra, M. Petrolo, E. Zappino. Finite Element Analysis of Structures through Unified Formulation. Wiley & Sons, Hoboken, New Jersey, USA. 2014.

[5] M. Enea, R. Augello, A. Pagani, E. Carrera. Global/local models of composite laminated structures coupling classical 2D finite elements and arbitrarily large refined analysis subdomains. Computers & Structures 298 (2024): 107368.

[6] E. Carrera, A. G. de Miguel, M. Filippi, I. Kaleel, A. Pagani, M. Petrolo, E. Zappino. Global-local plug-in for high-fidelity composite stress analysis in Femap/NX Nastran. Mechanics of Advanced Materials and Structures 28.11 (2021): 1121-1127.

[7] A. Pagani, A. R. Sánchez-Majano, M. Petrolo: Influence of structural theories on optimal fiber distributions in tow-steered composites considering local strain and stress. Aerotecnica Missili e Spazio (2025).

[8] H. Fukunaga and G. N. Vanderplaats, "Stiffness Optimization of Orthotropic Laminated Composites Using Lamination Parameters," AIAA Journal, vol. 29, no. 4, pp. 641–646, Apr. 1991. https://doi.org/10.2514/3.59931.

[9] H. Fukunaga, H. Sekine, M. Sato, and A. Iino, "Buckling design of symmetrically laminated plates using lamination parameters," Computers & Structures, vol. 57, no. 4, pp. 643–649, Nov. 1995. https://doi.org/10.1016/0045-7949(95)00050-Q.

[10] G. H. C. Silva, A. P. do Prado, P. H. Cabral, R. De Breuker, and J. K. S. Dillinger, "Tailoring of a Composite Regional Jet Wing Using the Slice and Swap Method," Journal of Aircraft, vol. 56, no. 3, pp. 990–1004, May 2019. https://doi.org/10.2514/1.C035094.

[11] MSC Software Corporation, "MSC Nastran 2023 Design Sensitivity and Optimization." 2023.

[12] H. Bau, D. Hoyt, and C. Rousseau, "Open Hole Compression Strength and Failure Characterization in Carbon/Epoxy Tape Laminates," in Composite Structures: Theory and Practice, P. Grant and C. Rousseau, Eds., 100 Barr Harbor Drive, PO Box C700, West Conshohocken, PA 19428-2959: ASTM International, 2001, pp. 273-273–20. https://doi.org/10.1520/STP14514S.

[13] W. J. Dorris, J. W. Hairr, J. T. Huang, J. E. Ingram, and B. M. Shah, "Advanced Composites Structural Concepts and Materials Technologies for Primary Aircraft Structures," p. 110.

[14] C. G. Diaconu and H. Sekine, "Layup Optimization for Buckling of Laminated Composite Shells with Restricted Layer Angles".

[15] J. L. Grenestedt and P. Gudmundson, "Layup Optimization of Composite Material Structures," in Optimal Design with Advanced Materials, Elsevier, 1993, pp. 311–336. https://doi.org/10.1016/B978-0-444-89869-2.50027-5.

[16] Kristin Marlett, "Hexcel 8552 IM7 Unidirectional Prepreg 190 gsm & 35% RC Qualification Material Property Data Report," Hexcel 8552 IM7 Uni Data Report Hexcel 8552 IM7 Uni Data Report CAM-RP-2009-015 Rev A, Apr. 2011.